Ligand–receptor binding revealed by the TNF family member TALL-1

Yingfang Liu*†, Xia Hong*†, John Kappler*‡§, Ling Jiang*, Rongguang Zhang||, Liangguo Xu*, Cheol-Ho Pan*, Wesley E. Martin*, Robert C. Murphy*, Hong-Bing Shu*¶, Shaodong Dai*‡ & Gongyi Zhang*§

* *Integrated Department of Immunology, National Jewish Medical and Research Center,* ‡ *Howard Hughes Medical Institute, and* § *Department of Pharmacology, Biomolecular Structure Program, School of Medicine, University of Colorado Health Science Center, 1400 Jackson Street, Denver, Colorado 80206, USA*
¶ *Department of Cell Biology and Genetics, College of Life Sciences, Peking University, Beijing 100871, China*
|| *Structural Biology Section, Argonne National Laboratory, 9700 South Cass Avenue, Argonne, Illinois 60439, USA*
† *These authors contributed equally to this work*

The tumour necrosis factor (TNF) ligand TALL-1 and its cognate receptors, BCMA, TACI and BAFF-R, were recently identified as members of the TNF superfamily, which are essential factors contributing to B-cell maturation. The functional, soluble fragment of TALL-1 (sTALL-1) forms a virus-like assembly for its proper function. Here we determine the crystal structures of sTALL-1 complexed with the extracellular domains of BCMA and BAFF-R at 2.6 and 2.5 Å, respectively. The single cysteine-rich domain of BCMA and BAFF-R both have saddle-like architectures, which sit on the horseback-like surface formed by four coil regions on each individual sTALL-1 monomer. Three novel structural modules, D2, X2 and N, were revealed from the current structures. Sequence alignments, structural modelling and mutagenesis revealed that one disulphide bridge in BAFF-R is critical for determining the binding specificity of the extracellular domain eBAFF-R to TALL-1 instead of APRIL, a closely related ligand of TALL-1, which was confirmed by binding experiments *in vitro*.

TNF family ligands and their corresponding receptors (TNF-Rs) have pivotal roles in many biological processes in mammalian cells, such as in host defence, inflammation, apoptosis, autoimmunity and organogenesis. At least 18 TNF ligands and 28 receptors have been identified so far. Some ligands have multiple receptors, and some receptors also bind multiple ligands. The interactions between ligands and receptors are usually very specific and have high affinity (0.1–1 nM)[1].

Ligands such as TALL-1/BAFF/THANK/BLyS/zTNF4 and APRIL/TALL-2, as well as receptors such as BCMA, TACI and BAFF-R/BR3, are recently identified members of the TNF/TNF-R family[2–15]. Overexpression of sTALL-1 in mice leads to increased numbers of mature B lymphocytes, spenomegaly, anti-DNA antibodies, proteinuria and glomerulonephritis. These phenotypes mimic those of SLE systemic lupus erythematosus[9–13]. TALL-1 deficiency in mice leads to the complete arrest of peripheral B cells at the T1 stage[16,17]. The phenotype is similar to that caused by BAFF-R deficiency[14,15]. The knockout of BCMA does not lead to any severe B-cell phenotypes[18]. It therefore seems that BCMA is dispensable for B-cell maturation. Knockout of TACI increased the total number of circulating B cells. However, the ratio of maturing B-cell subsets in the spleen was normal[19]. The role of TACI in the B-cell maturation process is still a mystery.

APRIL/TALL-2, the closest family member of TALL-1, has a low abundance in normal tissues but is present at high concentrations in transformed cell lines and in a variety of human cancers[20]. Recent data show that BAFF-R does not bind APRIL[14,15], suggesting that APRIL is dispensable for B-cell maturation[14,15,21]. Nevertheless, APRIL-deficient mice die *in utero*[22]. The role of APRIL is still unknown.

All other known structures of TNF ligands exist as trimers made entirely of β-strands and loops with a standard 'jellyroll' topology[23–28]. This is also true for sTALL-1 at low pH[29,30]. At pH 7.4 or higher, sTALL-1 forms a virus-like cluster through an unusual 'flap' region on sTALL-1 (ref. 31). Transfection and B-cell stimulation assays showed that this oligomerization status is required for its proper function[31].

The structure of the complex of TNF-β with cysteine-rich domains (CRDs) from its cognate receptor TNF-R1 has been determined[32]. This structure shows that the three elongated receptor domains bind to one TNF trimer at the interfaces formed between the TNF monomers[32]. Two CRDs (CRD2 and CRD3) make contacts with two distinct regions of TNF-β. The recently determined complex structure of TRAIL and DR5 disclosed a similar interaction mode to that observed in the TNF-β and TNF-R1 co-crystal structure, although CRD3 of DR5 assumes a different orientation from that in the TNF-β and TNF-R1 structures[33,34].

In contrast to the other receptor family members that have at least three or four CRDs in their extracellular domains, BAFF-R has only a half CRD (one module), BCMA has only one CRD, and TACI has two CRDs[6–9,14,15]. Nevertheless, the overall binding affinities of sTALL-1 with BCMA, BAFF-R and TACI are similar to those of other family members (0.1–1 nM)[31,35]. Furthermore, as predicted from sequence alignment, the CRDs in BCMA and TACI contain A1 and C2 modules[7], which are two of the multiply defined structural motifs that characterize the extracellular domains of TNF receptors[36]. The C2 module was also found in TNF-R1 and Fn14 (ref. 37). However, the C2 in TNF-R1 is not involved in ligand binding[36]. The only half CRD in BAFF-R was originally predicted to be the C2 module[14,15]. However, this CRD has recently been named as a new module, X2 (ref. 37). It is likely that there are novel interactions between these unique ligand–receptor couples that account for their high affinity[31,37]. In testing this hypothesis, we determine here the structures of sTALL-1 complexed with the extracellular domains of either BCMA (eBCMA) or BAFF-R (eBAFF-R).

Structural determination

Crystals of sTALL-1 with eBCMA and eBAFF-R were obtained by diffusing the receptor fragments into the sTALL-1 crystals (see Methods). The structures of both complexes were determined by difference Fourier analysis with the use of the available sTALL-1 model (Fig. 1a, Table 1 and Supplementary Information). The structure of sTALL-1 with eBCMA has been refined to an *R*-factor of 20.9% (R_{free}-factor 23.4%) against data to 2.6 Å resolution in space group $P6_122$, with 10 sTALL-1 monomers and seven complete molecules and one partial eBCMA molecule in the asymmetric unit

(unit cell 234 × 234 × 217 Å) (Table 1). Owing to crystal packing, another two receptor-binding sites were left unoccupied. Similar results are seen for the complex between sTALL-1 and eBAFF-R, with a final resolution of 2.5 Å (Table 1), although the corresponding partial eBAFF-R is almost completely disordered. The current model of the eBCMA monomer contains residues 5–43 (Fig. 1b). The model of eBAFF-R contains residues 16–45 (Fig. 1c).

Overall structure

The space group of the sTALL-1 crystals remained $P6_122$ with the same cell dimensions with or without receptors bound. There are two virus-like clusters in one unit cell. Each cluster has 60 copies of sTALL-1, 42 fully occupied eBCMA or eBAFF-R, and 6 partial copies of eBCMA or eBAFF-R. There are 12 copies of sTALL-1 free of receptors owing to crystal packing. All receptors are located on the outer extreme shell, which expands the ball-like shell another ~20 Å in each direction. The overall arrangement of the receptors on the shell looks like a sunflower, with receptors as the flower petals and sTALL-1 as the seedbed (Fig. 2). Molecules shown in red in Fig. 2 are missing from the complex structure; molecules shown in blue are partly occupied. The conformational change in sTALL-1 is negligible before and after receptor binding, which is the only similarity between this interaction and that of other TNF family members.

Four lines of evidence support the proposal that our crystal structure reflects the actual interactions of the complexes in solution and *in vivo*. First, coexpression of sTALL-1 with eBCMA or eBAFF-R generates the virus-like cluster in solution as judged by gel-filtration studies and SDS–polyacrylamide gel electrophoresis analysis at an approximate sTALL-1: eBCMA or sTALL-1:eBAFF-R ratio of 1:1. Different salt concentrations (from 100 mM to 1 M NaCl) produce the same elution profile, in which complexes of sTALL-1 with eBCMA or eBAFF-R are eluted at the void volume from a Superdex-200 column. Thus, binding between ligand and receptors is stable and insensitive to salt concentration. Second, in receptor-soaked sTALL-1 crystals, all seven fully occupied receptors and one partial receptor have equivalent binding sites on sTALL-1 in the asymmetric unit, so the binding is highly specific. Third, eBCMA and eBAFF-R have similar binding modes and occupy the same site on sTALL-1. Last, each of the three carboxy termini of eBCMA and eBAFF-R on the sTALL-1 trimer point in the same direction—towards the putative membrane surface for trimerization. Thus, we believe that the interactions revealed from the complex structures represent TALL-1–BCMA and TALL-1–BAFF-R *in vivo*.

Structure of eBCMA

As predicted, eBCMA contains two modules. One is the A1 module, consisting of three β-strands, with strands 1 and 3 linked by the only disulphide bridge[36]. The other module is C2-like (the two disulphide bridges formed are Cys III–Cys VI and Cys IV–Cys V), but the disulphide arrangement is the same as in a typical B2 module (the two disulphide bridges formed are Cys III–Cys V and Cys IV–Cys VI)[36] (Fig. 1b). For clarity, we temporarily termed this module D2 because of its difference from C2 and B2. There are two short helices in the D2 module that are located at the amino terminus and the C terminus of the module; one is from Cys III to Cys IV and the other is from Cys V to Cys VI. The latter helix extends further after the disulphide bridge and forms a helix three turns long, which is unique among all known TNF receptor structures. The arrangement of modules A1 and D2 of eBCMA is similar to that of A1 and C2 in

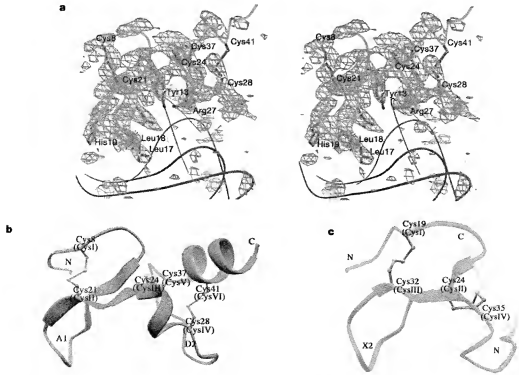

Figure 1 Structures of eBCMA and eBAFF-R. **a**, Initial $F_o - F_c$ map of eBCMA with sTALL-1 at the 2.5σ level. Phases are calculated from the sTALL-1 model (Protein Data Bank ID 1JH5). eBCMA is shown as the final refined model. The portion of the map shown is representative of all eight bound receptors in the asymmetric unit. Most residues are shown with their side chains. **b**, Ribbon diagram of the three-dimensional structure of eBCMA (residues 5–43), showing three disulphide bridges. **c**, Ribbon diagram of the three-dimensional structure of eBAFF-R (residues 16–45), showing two disulphide bridges. All figures were prepared with RIBBONS[44] except **a**, which was prepared with BOBSCRIPT[45].

Table 1 **Experimental data on crystal structure determination and refinement**

Data set	Resolution (Å)	R_{merge} (%)	No. of unique reflections	Total observations	Completeness (%)	*R*-factor	R_{free}	$\langle I/\sigma(I)\rangle$
eBCMA	2.6	12.9 (55.0)	97,672	1,056,960	94.0	20.9 (33.9)	23.5 (36.0)	10.9
eBAFF-R	2.5	13.5 (60.0)	121,940	1,415,809	99.3	24.5 (46.0)	26.9 (43.7)	14.4

$R_{merge} = \sum|I_i - \langle I\rangle| / \sum I_i$ with Bijvoet pairs treated as equivalent. Total observations are the number of full and partial observations measured with non-negative intensity to the indicated resolution. Completeness is the percentage of possible unique reflections measured with $I/\sigma(I) \geq -3$ (default value of SCALEPACK[29]) to the indicated resolution. *R*-factor= $\sum||F_o| - |F_c|| / \sum|F_o|$ for all amplitudes with $F_o/\sigma(F_o) > 0$ ($I/\sigma(I) \geq -3$) measured. R_{free} is calculated with 5% of the data. Data in parentheses are *R* values for the highest-resolution bins. $\langle I/\sigma(I)\rangle$ is the ratio of the average value of *I* to $\sigma(I)$. There is a total of 13,743 atoms in the final refinement for the eBCMA and sTALL-1 complex, and there is one water molecule, with r.m.s.d. bonds = 0.008 and r.m.s.d. angles = 1.56. There is a total of 13,230 atoms in the final refinement for the eBAFF-R and sTALL-1 complex, with r.m.s.d. bonds = 0.008 and r.m.s.d. angles = 1.7

TNF-R1 (ref. 36). Modules A1 and D2 form a saddle-like structure with each module as half of the saddle and the unique helix as the 'rider' (Fig. 1b). From the initial $2F_o - F_c$ and $F_o - F_c$ maps, all seven copies of the A1 modules are very rigid, with temperature factors similar to that of sTALL-1, and most side chains are ordered. The partial copy of the eighth eBCMA contains only the A1 module. The root-mean-square deviation (r.m.s.d.) is 0.2 Å for eight A1 modules in the asymmetry unit. In contrast, the D2 modules are relatively flexible, especially in the region between Cys IV and Cys V. The r.m.s.d. is 1.5 Å for the seven D2 modules in the asymmetry unit. The eighth D2 is severely disordered except for the region between Cys III and Cys IV.

Structure of eBAFF-R

To our surprise, most of eBAFF-R has a similar folding to that of eBCMA, although it was predicted that eBAFF-R contains only one C2 or X2 module[14,15,37] (Fig. 1c). The structure of eBAFF-R shows that it contains one major module, X2, and one minor N-shaped module (with no disulphide bridge), which we temporarily named module N. The X2 module contains four cysteines, which form two disulphide bridges. The X2 module is similar to the A1 model in eBCMA, but the additional disulphide bridge is typical of the B2 instead of the A2 module. We temporarily named this module X2, following the name from the literature[37]. For the N module, there is a one-turn helix and a coil eight residues long. Interestingly, from the initial $2F_o - F_c$ and $F_o - F_c$ maps, the coil region is well ordered, although it does not seem to make any contact with the other part of eBAFF-R. We believe that the three proline residues in the coil region account for this rigidity. We conclude that BAFF-R has the smallest functional motif in its extracellular part among all known TNF receptor members. A partial model of BAFF-R derived from NMR spectra has a similar structural feature to part of the X2 module[38].

Comparison of eBCMA with eBAFF-R

The sequence homology between eBCMA and eTACI (the extracellular domain of TACI) is obvious, in contrast to that between eBCMA and eBAFF-R or between eTACI and eBAFF-R. As mentioned above, eBCMA and eBAFF-R have a similar saddle-like fold. Judged by structure superposition, the A1 module from eBCMA and the X2 module from eBAFF-R (with a r.m.s.d. of 0.6 Å) are almost identical (Fig. 3a, b). Although we could not find a corresponding D2 module in eBAFF-R for comparison, the initial one-turn helix motifs in both D2 of eBCMA and the N module of eBAFF-R are identical. This is also true for the C2 module of TNF-R1 (Fig. 3c). The major difference between eBCMA and eBAFF-R occurs after the one-turn helix. The lone extended coil in eBAFF-R contrasts with other typical TNF receptor structural modules (Fig. 3a).

The structures of eBCMA and eBAFF-R allowed us to perform a structure-based sequence alignment of eBCMA, eBAFF-R, eTACI and C2 of TNF-R1. A strong pattern of similarity emerged from this comparison (Fig. 3d). The high sequence similarities between the two CRDs in TACI and CRDs in BCMA suggest that each CRD of TACI contains one A1 module and one D2 module. Another TNF receptor member, Fn14, which also contains one CRD, was predicted to contain one A1 module and one C2 module[37]. From our sequence-alignment result, Fn14 could contain either D2 or C2 (Fig. 3d). The ambiguity will only be resolved by a structural determination of this module. Nevertheless, we speculate that the

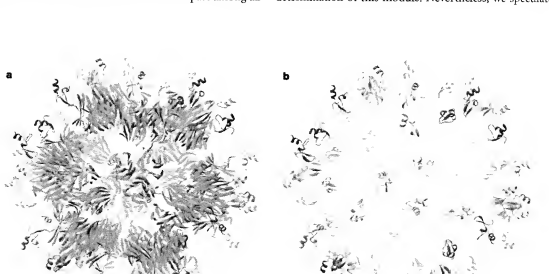

Figure 2 Overall structure of eBCMA with or without sTALL-1. **a**, The 60 monomers of sTALL-1 (green) and 60 monomers of eBCMA (molecules coloured yellow exist in the structure, molecules coloured blue are partly ordered, and molecules coloured red are missing from the complex owing to crystal packing). **b**, As **a**, but without sTALL-1.

interaction mode between Fn14 and its ligand TWEAK are similar to what we found in the complexes of eBCMA and eBAFF-R with sTALL-1 (see below).

Interactions of sTALL-1 and eBCMA

The interactions between sTALL-1 and eBCMA are mostly in a one-to-one mode—one monomer of the receptor to one monomer of the ligand. The slightly tilted saddle-like receptor is sitting on a horse-back-like surface. This surface is formed by four loops from the ligand (the two connecting strands GH and A′A on one side and the other two connecting strands CD and EF on the other; Fig. 4a, b). This mode of interaction is markedly different from that seen within other TNF family members, in which one elongated receptor binds

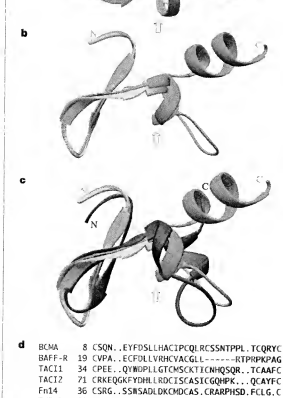

d

BCMA	8	CSQN..EYFDSLLHACIPCQLRCSSNTPPL.TCQRYC	41
BAFF-R	19	CVPA..ECFDLLVRHCVACGLL-----RTPMPKPAG	47
TACI1	34	CPEE..QYWDPLLGTCMSCKTICNHQSQR..TCAAFC	66
TACI2	71	CRKEQGKFYDHLLRDCISCASICGQHPK...QCAYFC	104
Fn14	36	CSRG..SSHSADLDKCMDCASC.CRARPHSD.FCLG.C	67
TNF-R1	168	CHNG....FFLKGAKCISCHD.CKN.....KECEKLC	194

Figure 3 Comparison of different CRDs. **a**, Superposition of eBCMA (green) and eBAFF-R (yellow). **b**, Rotation of **a** through 90° **c**, Superposition of eBCMA, eBAFF-R and the C2-containing CRD from TNF-R1 (ref. 36). **d**, Structure-based sequence alignment of CRD modules of BCMA, BAFF-R, TACI, Fn14 and TNF-R1. Residues coloured red are conserved disulphide bridges, which form modules A1, X2, D2 and C2. There is no structural similarity to other members after Leu 38 for eBAFF-R. Residues coloured blue are involved in ligand binding. Arrows indicate the one-turn helix in the N module.

to the cleft formed by two ligands (Supplementary Information). The interactions of eBCMA with sTALL-1 include hydrogen bonds, salt bridges and, most importantly, hydrophobic contacts with a contact distance of between 3 and 4 Å. A total of 21 residues are involved: 9 from eBCMA (Tyr 13, Asp 15, Leu 17, Leu 18, His 19, Ile 22, Leu 26, Arg 27 and Pro 34), 8 from the primary ligand (Tyr 163, Tyr 206, Leu 211, Arg 231, Ile 233, Pro 264, Arg 265 and Glu 266) and 4 from the secondary ligand (Leu 200, Leu 240, Asp 273 and Asp 275) of the trimer (Fig. 4c–f). The overall interactions can be divided into four groups. First, Leu 17 and Leu 18 from eBCMA, together with Tyr 163, Leu 211, Ile 233 and Pro 264 from the primary ligand and Leu 200 from the secondary ligand, form the first hydrophobic core (Fig. 4d). Tyr 163, Leu 200, Ile 233 and Pro 264 are located on a curved track. Together with Leu 17 from eBCMA, these residues form a perfect hydrophobic curved track. Leu 211 from the primary ligand and Leu 18 from eBCMA strengthen the contacts further (Fig. 4d). Second, Ile 22 and Leu 26 from eBCMA, together with Tyr 206 from the primary ligand and Leu 240 from the secondary ligand, form the second hydrophobic core (Fig. 4e). Third, Asp 15 from eBCMA and Arg 265 from the primary ligand form one salt bridge, and Arg 27 from eBCMA and Glu 266 from the primary ligand form another (Fig. 4f). There is also a potential hydrogen bond between Tyr 206 from the primary ligand and Tyr 13 from eBCMA (Fig. 4f). Last, His 19 from eBCMA forms one water-molecule-mediated interaction with Arg 231 of the primary ligand (Fig. 4d). Twenty per cent of the sTALL-1 exposed surface (3,696 $Å^2$ of the 17,868-$Å^2$ sTALL-1 trimer surface) and 38% of the eBCMA surface (1,232 $Å^2$ of the 3,237-$Å^2$ eBCMA monomer surface) are involved in the interaction.

Interactions of sTALL-1 and eBAFF-R

Most interactions between sTALL-1 and eBAFF-R are similar to those between sTALL-1 and eBCMA, although the details vary. The interactions also include hydrogen bonds, salt bridges and hydrophobic contacts. There are 24 residues involved in total: 9 from eBAFF-R (Asp 26, Leu 28, Val 29, Arg 30, Val 33, Leu 37, Leu 38, Arg 39 and Arg 42), 10 from the primary ligand (Tyr 163, Asp 203, Tyr 206, Leu 211, Arg 231, Ile 233, Pro 264, Arg 265, Glu 266 and Asn 267), 4 from the secondary ligand (Leu 200, Leu 240, Asp 273 and Asp 275), and 1 from a flap region of the neighbouring trimer (Asp 222) (Fig. 4g–i). The overall interactions also can be divided into four groups. First, Leu 28 and Val 29 from eBAFF-R, together with Tyr 163, Leu 211, Ile 233 and Pro 264 from the primary ligand and Leu 200 from the secondary ligand, form the first hydrophobic core (Fig. 4g). In comparison with eBCMA, Val 29 in eBAFF-R replaces the equivalent Leu 18. The side chain is shortened, and this could reduce the strength of the contact. Second, Val 33, Leu 37 and Leu 38 from eBAFF-R, together with Tyr 206 from the primary ligand and Leu 240 from the secondary ligand, form the second hydrophobic core (Fig. 4h). Val 33 and Leu 37 in eBAFF-R are equivalent to Ile 22 and Leu 26 in eBCMA. Leu 38 is an additional contacting residue for eBAFF-R compared with eBCMA. Third, Asp 26 from eBAFF-R and Arg 265 from the primary ligand form a salt bridge (not shown). The replacement of Arg 27 in eBCMA with Leu 38 in eBAFF-R eliminates a salt bridge with Glu 266 from the primary ligand. However, Leu 38 joins the second hydrophobic core, which might strengthen the interaction between eBAFF-R and sTALL-1 (Fig. 4h). Last, Arg 30 from eBAFF-R, Arg 231 from the primary ligand, Asp 273 and Asp 275 from the secondary ligand and Asp 222 from the third ligand form a complicated salt bridge network (Fig. 4g). The long side chain of Arg 30 from eBAFF-R (His 19 in eBCMA; Fig. 4d) makes contacts with either Asp 275 or Asp 222. The well-defined electron density of the Arg 30 side chain from eBAFF-R in the initial difference maps suggests that these are strong interactions that might considerably strengthen the eBAFF-R and sTALL-1 binding. In addition, there are three interactions over the extended coil region of eBAFF-R, which might also have a

crucial role in keeping the coil region in an ordered form in the structure. First, Arg 39 makes a salt bridge with Asp 203 of the primary ligand. Second, Arg 42 from eBAFF-R forms a hydrogen bond with Asn 267 from the primary ligand. Last, Glu 266 from the primary ligand makes one hydrogen bond with the main chain of the coil (Fig. 4i). In contrast, Glu 266 and Arg 27 of eBCMA make a salt bridge in the complex of eBCMA with sTALL-1 (Fig. 4f). Overall, 23% of the exposed surface of sTALL-1 (4,197 Å^2 of the 17,868-Å^2 sTALL-1 trimer surface) and 44.8% of the eBAFF-R surface (1,399 Å^2 of the 3,121-Å^2 eBAFF-R monomer surface) are involved in the interaction. Furthermore, eBAFF-R occupies more surface than eBCMA does on sTALL-1.

Discrimination of BAFF-R between APRIL and TALL-1

The two publications that initially reported the cloning of the BAFF-R/BR3 receptor found that BAFF-R specifically binds to TALL-1 but not to APRIL/TALL-2 (refs 14, 15). Furthermore, APRIL has a very low abundance in all tissues, and was proposed to be dispensable for B-cell maturation[20,21]. It has also been predicted that there might be an additional and more specific receptor for APRIL[39]. The binding affinities of APRIL for eBCMA and eTACI are similar to those of sTALL-1 for eBCMA and eTACI[25]. From the above structural analysis, eBCMA and eBAFF-R have nearly identical core structures that make contacts with sTALL-1. Furthermore, the interactions between eBCMA and sTALL-1 are also highly conserved in the interactions between eBAFF-R and sTALL-1. We speculate that these interactions are also conserved for TACI and sTALL-1. Given these structural similarities, why should BAFF-R discriminate between TALL-1 and APRIL? To address this question, we modelled APRIL on the basis of the sTALL-1 structure (see Methods and Supplementary Information), benefiting from the high primary-sequence homology between sTALL-1 and APRIL[7]. The final coordinates of APRIL were superimposed on the sTALL-1 structure (Fig. 5a). Detailed interactions between eBAFF-R and APRIL were analysed. To our surprise, the interactions are extremely similar to those found in the complexes between eBCMA or eBAFF-R and sTALL-1. The first hydrophobic core we described in the two previous complexes still exists, including Leu 28 and Val 29 from eBAFF-R, Val 133, Thr 177, Val 181, Ile 197 and Pro 230 from the primary APRIL molecule, and Leu 170 from the secondary

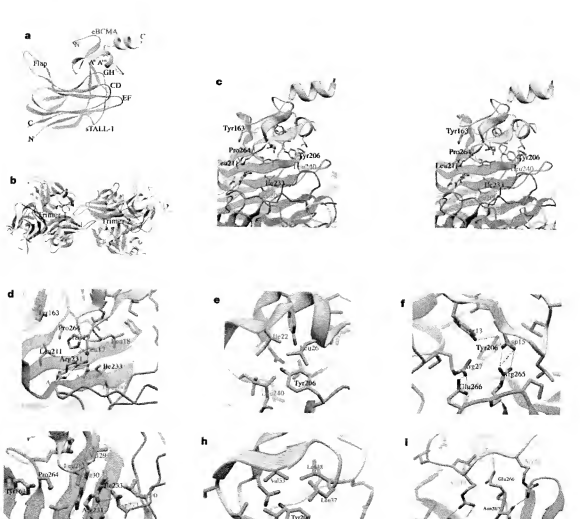

Figure 4 Detailed interactions of the two complexes. **a**–**f**, Interactions between eBCMA and sTALL1: **a**, the one-to-one interaction mode of eBCMA with sTALL-1; **b**, two trimers of the complex of eBCMA and sTALL-1; **c**, the overall interactions between eBCMA and sTALL-1; **d**, hydrophobic core 1 between eBCMA and sTALL-1; **e**, hydrophobic core 2 between eBCMA and sTALL-1; **f**, salt bridges 1 and 2 in the complex of eBCMA and sTALL-1. **g**–**i**, Interactions between eBAFF-R and sTALL-1: **g**, hydrophobic core 1 between eBAFF-R and sTALL-1; **h**, hydrophobic core 2 between eBAFF-R and sTALL-1; **i**, hydrogen bonds and salt bridges in the extended coil region of eBAFF-R with sTALL-1.

APRIL molecule (not shown). The second hydrophobic core consists of Val 33, Leu 37, Leu 38 from eBAFF-R, Phe 176 from the primary ligand, and Arg 206 from the secondary ligand (not shown). In comparison with the interactions between eBAFF-R and sTALL-1, Tyr 206 from the primary ligand is changed to Phe 176; Leu 240 from the secondary ligand is changed to Arg 206. The former change could strengthen the hydrophobic contacts. Additionally, the major salt bridge formed by Asp 26 from the receptor and Arg 195 from APRIL is conserved (not shown). Thus, we seek the structural basis of eBAFF-R's discrimination between TALL-1 and APRIL.

To find this basis, a serial truncation, a point mutation and a combination of both were introduced (Fig. 5b). All protein versions with the above mutations were subjected to BIAcore binding assays to measure their binding affinity to sTALL-1 and APRIL. To obtain the true affinity of the receptor without the compounding effect of multivalent binding, the polyvalent sTALL-1 proteins and APRIL were immobilized in the flow cells of the instrument, and soluble monomeric eBAFF-R and its derivatives were injected in the mobile phase. The K_d values of the interaction were calculated from the kinetic binding data. We found only one version of eBAFF-R truncation (eBAFF-R(1–36), with a complete C-terminal truncation starting from residue 37) with significant binding affinity for APRIL (Fig. 5b, c). This fragment contains only the X2 module.

These results also can be mimicked by energy minimization of models. When interaction models of APRIL and eBAFF-R are subjected to energy minimization in CNS[40], eBAFF-R is pushed away from APRIL by about 0.5 Å. This did not occur when only the X2 module was included in the process. It seems that the C-terminal half of the eBAFF-R molecule (module N) has an inhibitory role in the binding of eBAFF-R to APRIL.

The failure of eBAFF-R(1–39) to bind to APRIL (Fig. 5b) suggests that some features of residues 37–39 are important for the inhibition of binding. We therefore examined this region in eBAFF-R and eBCMA, because they are bound to sTALL-1 and we model them bound to APRIL (Fig. 5d, e). Although APRIL and sTALL-1 are structurally similar in the hydrophobic core, the microenvironment is slightly different. The aromatic side chain of Phe 176 in

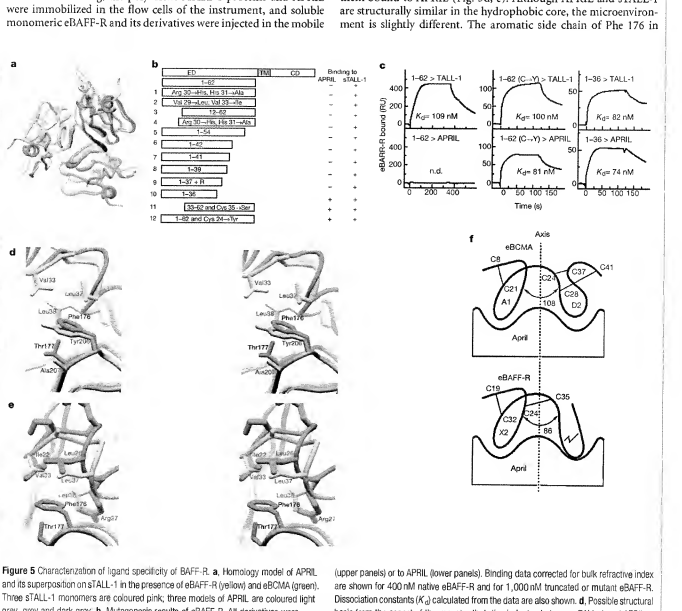

Figure 5 Characterization of ligand specificity of BAFF-R. **a**, Homology model of APRIL and its superposition on sTALL-1 in the presence of eBAFF-R (yellow) and eBCMA (green). Three sTALL-1 monomers are coloured pink; three models of APRIL are coloured light grey, grey and dark grey. **b**, Mutagenesis results of eBAFF-R. All derivatives were subjected to binding assays on APRIL with sTALL-1 as a positive control. **c**, Binding of eBAFF-R and its derivatives to sTALL-1 and APRIL. As described in Methods, surface plasmon resonance was used to assess the binding of native eBAFF-R(1–62), Cys 24 → Tyr 24 mutated eBAFF-R and truncated eBAFF-R(1–36) to immobilized sTALL-1 (upper panels) or to APRIL (lower panels). Binding data corrected for bulk refractive index are shown for 400 nM native eBAFF-R and for 1,000 nM truncated or mutant eBAFF-R. Dissociation constants (K_d) calculated from the data are also shown. **d**, Possible structural basis from the aspect of the receptor that discriminates between sTALL-1 and APRIL. Different proteins are coloured as follows: eBCMA, green; eBAFF-R, yellow; sTALL-1, pink; APRIL, dark grey. **e**, Possible structural basis from the aspect of the ligand that discriminates between sTALL-1 and APRIL, coloured as in **d**. **f**, A model of how eBAFF-R differentiates sTALL-1 from APRIL.

APRIL is predicted to be above the corresponding residue Tyr 206 in sTALL-1, which could clash with the side chain of Leu 38 in eBAFF-R (Fig. 5d). In addition, in APRIL the side chain of Thr 177 could restrict the mobility of the aromatic ring of Phe 176. This is in contrast to the more freedom given to Tyr 206 in sTALL-1 by Ala 207. From the aspect of the receptor, the one-turn helix in module N of eBAFF-R is much lower than that in eBCMA. This could lead to a repulsive contact between the one-turn helix region in eBAFF-R and Phe 176 in APRIL (Figs 3a–c and 5e).

A structural comparison between eBCMA and eBAFF-R further reveals that the unique disulphide bridge (Cys 24–Cys 35) in the X2 module creates an additional connection between modules X2 and N, which eliminates the flexibility between the two modules in eBAFF-R (Fig. 5f). On the one hand, this change pulls the two modules closer in eBAFF-R (from ~108° in eBCMA to ~86° in eBAFF-R; Fig. 5f); on the other hand, it eliminates the possibility of subtle conformation adjustment during the protein–protein recognition process because of the rigidity between two modules (Fig. 5f). To test whether the disulphide is the key component in inhibiting the binding of eBAFF-R to APRIL, we generated two point mutations, Cys 24 → Tyr 24 (the corresponding residue in eBCMA is Tyr) and Cys 35 → Ser 35. Both mutants, which cannot form the disulphide, turned out to have similar binding affinities for both sTALL-1 and APRIL (Fig. 5b, c).

Although the module N in eBAFF-R has an inhibitory role in the binding process of eBAFF-R to APRIL, we believe that module N alone should bind to sTALL-1 and APRIL, because it can freely adapt its orientation to obtain the best fit without the restraint of the disulphide bridge. A slightly modified module N of eBAFF-R (residues 33–62 and Cys 35 → Ser 35; Fig. 5b) does bind to both sTALL-1 and APRIL (data not shown). In conclusion, the above analysis reveals that the unique disulphide bridge in eBAFF-R, which restricted mobility between the X2 and N modules, is the only determinant that prevents eBAFF-R from binding to APRIL.

We have previously speculated that APRIL could have a role as a decoy ligand[31]. From the modelling results, we also found that residues involved in trimerization are absolutely conserved (data not shown). This information suggested that sTALL-1 and APRIL are expressed in the same environment and that they could simultaneously form heterotrimers. Patients with autoimmune diseases do indeed have detectable heterotrimers of sTALL-1 and APRIL in their circulation[41]. As we concluded previously, the sTALL-1 trimer alone (mTALL-1) is unable to trigger the signal transduction of its cognate receptors[31]. Heterotrimers of sTALL-1 and APRIL cannot form a virus-like cluster, as sTALL-1 alone does, owing to the lack of the 'flap' region in APRIL. We think it significant that heterotrimers of sTALL-1 and APRIL have an even higher activity than sTALL-1 alone, as reported previously[41]. Considering the fact that overexpression of sTALL-1 could lead to an abnormal stimulation of B cells and the development of autoimmune disease, APRIL might be serving as a balancer, reducing the opportunity for excess sTALL-1 to form the active cluster. This role is similar to the decoy death receptors, which are essential for cells to survive[27,33,34]. Knockout data show that such mice lacking APRIL die at early embryonic stages—indirect evidence of the potentially important roles of this protein[32]. □

Methods

Protein expression, purification and crystallization

Protein expression, purification and crystallization of sTALL-1 have been described previously[31]. BAFF-R/BR3 was cloned as described[14,15]. The extracellular domains of BCMA(1–54), BAFF-R(1–62) and other BAFF-R derivatives used for the experiments were overexpressed as glutathione *S*-transferase (GST) fusion proteins on pGEX4T-2 vector in *Escherichia coli* strain BL-21 (ref. 31). Cell preparation and protein purification procedures were similar to that of sTALL-1. In brief, harvested cells were lysed with a French press and subjected to low-speed centrifugation. The soluble fraction was loaded on GST-affinity beads. After an extensive wash with binding buffer, thrombin was added and incubated for 24 h. The supernatant containing the extracellular domains of BCMA and BAFF-R were loaded on a MonoQ column and eluted with a NaCl gradient. The protein was more than 99% pure after the MonoQ step.

Structural determination and refinement

For complex crystal preparations, sTALL-1 crystals were harvested after 2 weeks. sTALL-1 crystals were transferred to a stable soaking solution containing 40% dioxane, the corresponding receptors at 1 mM, and 100 mM Bicine, pH 9.0. After being soaked overnight, crystals were transferred to the cryoprotecting buffer system used for sTALL-1 crystals[31]. Data sets for both complexes were first collected on the in-house X-ray generator. Crystals of both complexes diffracted to 3.0 Å. A 2.6-Å data set for the complex of eBCMA with sTALL-1 and a 2.5-Å data set for the complex of eBAFF-R with sTALL-1 were collected at the Advanced Photon Source (APS) facility. All data were processed with the DENZO package[45]. Structures of the complexes were solved by difference Fourier analysis with the use of the sTALL-1 model[31]. After one round of minimization of the sTALL-1 model in CNS[46], $2F_o - F_c$ and $F_o - F_c$ maps were calculated. Models were built using O (ref. 43) and refined in CNS. CRDB (containing modules A1 and C2) of TNF-R1 (Protein Data Bank ID 1NCF) was used for initial model building of eBCMA. Model building of eBAFF-R was helped by the available model of eBCMA (Supplementary Information).

Model building of APRIL

The most obvious difference between sTALL-1 and APRIL is in the 'flap' region (six residues) of sTALL-1, which APRIL lacks[1]. We reported a mutated version of sTALL-1, with eight residues replaced by two glycine residues, that was not functional in transfection assays or in the B-cell stimulation assays but had a binding affinity to its receptors similar to that of native sTALL-1 (ref. 31). This mutated sTALL-1 is a good model for APRIL. The structure of this mutated sTALL-1 has been determined at 1.7 Å resolution by multiple isomorphous replacement; it is almost identical to that of sTALL-1, except for the missing 'flap' (Supplementary Information). In accordance with the sequence alignment result[1], the APRIL residues were mutated manually in O. The side chains of all APRIL residues were orientated as for the corresponding ones in sTALL-1. Two regions with one or two residue insertions were built automatically with O (main chain auto-building mode). The final model of APRIL was imported into the minimization program in CNS.

Protein binding assays

Wild-type multimeric sTALL-1 and APRIL (R&D Systems) were immobilized (~5,000 resonance units (RU) of each) in separate flow cells of a CM-5 Biacore biosensor chip by using standard amine-coupling reagents. Various concentrations (100–2,000 nM) of monomeric eBAFF-R or its derivatives in a buffer containing 250 mM NaCl, 50 mM Tris buffer, pH 8.0, 20 mM EDTA and 0.005% P20 detergent were injected for 2–5 min at a flow rate of 25 µl min^{-1}, and the binding kinetics were recorded. To correct for bulk refractive index, eBAFF-R and its derivative samples were injected into a control flow cell with no protein immobilized. Association and dissociation rates were calculated with standard Biacore software (BIAevaluation 3.0). For both sTALL-1 and APRIL experiments, the model A + B ⇌ AB and the fitting option correcting for mass transport effects were used.

Received 27 January; accepted 11 March 2003; doi:10.1038/nature01543.

1. Locksley, R. M., Killeen, N. & Lenardo, M. J. The TNF and TNF receptor superfamilies: integrating mammalian biology. *Cell* **104,** 487–501 (2001).
2. Shu, H. B., Hu, W. H. & Johnson, H. TALL-1 is a novel member of the TNF family that is downregulated by mitogens. *J. Leukocyte Biol.* **65,** 680–683 (1999).
3. Schneider, P. *et al.* BAFF, a novel ligand of the tumour necrosis factor family, stimulates B cell growth. *J. Exp. Med.* **189,** 1747–1756 (1999).
4. Moore, P. A. *et al.* BLyS: member of the tumour necrosis factor family and B lymphocyte stimulator. *Science* **285,** 260–263 (1999).
5. Mukhopadhyay, A., Ni, J., Zhai, Y., Yu, G. L. & Aggarwal, B. B. Identification and characterization of a novel cytokine, THANK, a TNF homologue that activates apoptosis, nuclear factor-κB, and c-Jun NH$_2$-terminal kinase. *J. Biol. Chem.* **274,** 15978–15981 (1999).
6. Shu, H. B. & Johnson, H. B cell maturation protein is a receptor for the TNF family member TALL-1. *Proc. Natl Acad. Sci. USA* **97,** 9156–9161 (2000).
7. Gross, J. A. *et al.* TACI and BCMA are receptors for a TNF homologue implicated in B cell autoimmune disease. *Nature* **404,** 995–999 (2000).
8. Thompson, J. S. *et al.* BAFF binds to the tumour necrosis factor receptor-like molecule B cell maturation antigen and is important for maintaining the peripheral B cell population. *J. Exp Med* **192,** 129–135 (2000).
9. Marsters, S. A. *et al.* Interaction of the TNF homologues BLyS and APRIL with the TNF receptor homologues BCMA and TACI. *Curr. Biol.* **10,** 785–788 (2000).
10. Xia, X. Z. *et al.* TACI is a TRAF-interacting receptor for TALL-1, a tumour necrosis factor family member involved in B cell regulation. *J. Exp. Med.* **192,** 137–143 (2000).
11. Yan, M. *et al.* Identification of a receptor for BLyS demonstrates a crucial role in humoral immunity. *Nature Immunol.* **1,** 37–41 (2000).
12. Mackay, F. *et al.* Mice transgenic for BAFF develop lymphocytic disorders along with autoimmune manifestations. *J. Exp. Med.* **190,** 1697–1710 (1999).
13. Khare, S. D. *et al.* Severe B cell hyperplasia and autoimmune disease in TALL-1 transgenic mice. *Proc Natl Acad. Sci. USA* **97,** 3370–3375 (2000).
14. Thompson, J. S. *et al.* BAFF-R, a novel TNF receptor that specifically interacts with BAFF. *Science* **293,** 2108–2111 (2001).
15. Yan, M. *et al.* Identification of a novel receptor for B lymphocyte stimulator that is mutated in a mouse strain with severe B cell deficiency. *Curr. Biol.* **11,** 1547–1552 (2001).
16. Schiemann, B. *et al.* An essential role for BAFF in the normal development of B cells through a BCMA-independent pathway. *Science* **293,** 2111–2114 (2001).
17. Gross, J. A. *et al.* TACI-Ig neutralizes molecules critical for B-cell development and autoimmune disease. Impaired B-cell maturation in mice lacking BLyS. *Immunity* **15,** 289–302 (2001).

18. Xu, S. & Lam, K.-P. B-cell maturation protein, which binds the tumour necrosis factor family members BAFF and APRIL, is dispensable for humoral immune response. *Mol. Cell. Biol.* **21,** 4067–4074 (2001).
19. Von Bulow, G. U., van Deursen, J. M. & Bram, R. J. Regulation of the T-independent humoral response by TACI. *Immunity* **14,** 573–582 (2001).
20. Hahne, M. *et al.* APRIL, a new ligand of the tumor necrosis factor family, stimulates tumor cell growth. *J. Exp. Med.* **188,** 1185–1190 (1998).
21. Schneider, P. *et al.* Maturation of marginal zone and follicular B cells requires B cell activation factor of the tumour necrosis factor family and is independent of B cell maturation antigen. *J. Exp. Med.* **194,** 1691–1697 (2001).
22. Mackay, F. & Mackay, C. R. The role of BAFF in B-cell maturation, T-cell activation and autoimmunity. *Trends Immunol.* **23,** 113–115 (2002).
23. Jones, E. Y., Stuart, D. I. & Walker, N. P. Structure of tumour necrosis factor. *Nature* **338,** 225–228 (1989).
24. Eck, M. J. & Sprang, S. R. The structure of tumour necrosis factor-α at 2.6 Å resolution: implications for receptor binding. *J. Biol. Chem.* **264,** 17595–17605 (1989).
25. Eck, M. J., Ultsch, M., Rinderknecht, E., de Vos, A. M. & Sprang, S. R. The structure of human lymphotoxin (tumour necrosis factor β) at 1.9 Å resolution. *J. Biol. Chem.* **267,** 2119–2122 (1992).
26. Karpusas, M. *et al.* 2 Å crystal structure of an extracellular fragment of human CD40 ligand. *Structure* **3,** 1031–1039 (1995).
27. Cha, S. S. *et al.* 2.8 Å resolution crystal structure of human TRAIL, a cytokine with selective antitumor activity. *Immunity* **11,** 253–261 (1999).
28. Lam, J., Nelson, C. A., Ross, F. P., Teitelbaum, S. L. & Fremont, D. H. Crystal structure of the TRANCE/RANKL cytokine reveals determinants of receptor–ligand specificity. *J. Clin. Invest.* **108,** 971–979 (2001).
29. Karpusas, M. *et al.* Crystal structure of extracellular human BAFF, a TNF family member that stimulates B lymphocytes. *J. Mol. Biol.* **315,** 1145–1154 (2002).
30. Oren, D. A. *et al.* Structural basis of BlyS receptor recognition. *Nature Struct. Biol.* **9,** 288–292 (2002).
31. Liu, Y. *et al.* Crystal structure of sTALL-1 reveals a virus-like assembly of TNF family ligands. *Cell* **108,** 383–394 (2002).
32. Banner, D. W. *et al.* Crystal structure of the soluble human 55 kd TNF receptor–human TNF complex: implications for TNF receptor activation. *Cell* **73,** 431–445 (1993).
33. Mongkolsapaya, J. *et al.* Structure of the TRAIL–DR5 complex reveals mechanisms conferring specificity in apoptotic initiation. *Nature Struct. Biol.* **6,** 1048–1053 (1999).
34. Hymowitz, S. G. *et al.* Triggering cell death: the crystal structure of Apo2L/TRAIL in a complex with death receptor 5. *Mol. Cell* **4,** 563–571 (1999)
35. Yu, G. *et al.* APRIL and TALL-I and receptors BCMA and TACI: system for regulating humoral immunity. *Nature Immunol.* **1,** 252–256 (2000).
36. Naismith, J. H. & Sprang, S. R. Modularity in the TNF-receptor family. *Trends Biochem. Sci.* **23,** 74–79 (1998).
37. Bodmer, J. L., Schneider, P. & Tschopp, J. The molecular architecture of the TNF superfamily. *Trends Biochem. Sci.* **27,** 19–26 (2002).
38. Kayagaki, N. *et al.* BAFF/BlyS receptor 3 binds the B cell survival factor BAFF ligand through a discrete surface loop and promotes processing of NF-κB2. *Immunity* **17,** 515–524 (2002).
39. Ware, C. F. APRIL and BAFF connect autoimmunity and cancer. *J. Exp. Med.* **192,** F35–F37 (2000).
40. Brunger, A. T. *et al.* Crystallography and NMR System (CNS): A new software system for macromolecular structure determination. *Acta Crystallogr. D* **54,** 905–921 (1998).
41. Roschke, V. *et al.* BlyS and APRIL form biologically active heterotrimers that are expressed in patients with systemic immune-based rheumatic diseases. *J Immunol.* **169,** 4314–4321 (2002)
42. Otwinowski, Z. & Minor, W. Processing X-ray diffraction data collected in oscillation mode. *Methods Enzymol.* **276,** 307–326 (1997).
43. Jones, T. A., Zou, J. Y., Cowan, S. & Kjeldgaard, A. L. Improved methods for building protein models in electron density maps and the location of errors in these models. *Acta Crystallogr. A* **47,** 110–119 (1991).
44. Carson, M. Ribbon models of macromolecules. *Methods Enzymol.* **277,** 493–505 (1997).
45. Esnouf, R. M. BobScript v2.4 changes (C). *J. Mol. Graphics* **15,** 132–134 (1997).

Supplementary Information accompanies the paper on **www.nature.com/nature.**

Acknowledgements We thank R. Zhao, O. Swartz and L. Halton for reading our manuscript; Z. Chen for Fig. 5f; M. Carson, S. R. Sprang, C. R. Mackay and J. Tschopp for their suggestions; the Howard Hughes Medical Institute, Zuckerman/Canyon Ranch and A. Lapporte for the support of our X-ray and computing facility; A. Joachimiak and SBC (ID-19) at APS for high-resolution data; and P. C. Marrack, J. D. Crapo, J. Cambier, X. Liu and other members at the National Jewish Medical and Research Center for support. S.H.B. is supported by an NIH grant and the Arthritis Foundation; Y.L. is supported partly by a Priscilla Campbell Memorial Fellowship; X.H. is supported partly by a Janet S. Lewald fellowship; G.Z. is supported by a PEW Scholar Award, a start-up fund from National Jewish Medical and Research Center and the Cancer League of Colorado, Inc.; P.M. and G.Z. are supported by NIH grants.

Competing interests statement The authors declare that they have no competing financial interests.

Correspondence and requests for materials should be addressed to G.Z. (zhangg@njc.org). The atomic coordinates and reflections have been deposited in the Protein Data Bank under accession codes 1OQD and 1OQE.